Intensity and source state dependence of the quasi-periodic oscillations in Scorpius X-1

van der Klis, M.; Stella, L.; White, N.; Jansen, F.; Parmar, A.N.

DOI
10.1086/165210

Publication date
1987

Published in
Astrophysical Journal

THE ASTROPHYSICAL JOURNAL, 316:411–426, 1987 May 1

INTENSITY AND SOURCE STATE DEPENDENCE OF THE QUASI-PERIODIC OSCILLATIONS IN SCORPIUS X-1

M. VAN DER KLIS, L. STELLA,[1] AND N. WHITE
EXOSAT Observatory, Astrophysics Division, Space Science Department of ESA, ESTEC
F. JANSEN
Laboratory for Space Research, Leiden
AND
A. N. PARMAR
EXOSAT Observatory, Astrophysics Division, Space Science Department of ESA, ESTEC
Received 1986 May 21; accepted 1986 October 22

ABSTRACT

Following the discovery with *EXOSAT* of intensity-dependent 20–40 Hz quasi-periodic oscillations (QPO) from GX 5−1, similar oscillations at 6 Hz were discovered from *EXOSAT* observations of Sco X-1 in its quiescent state by Middleditch and Priedhorsky. We report here on the properties of the QPO seen in earlier *EXOSAT* observations of Sco X-1. During these observations QPO were also detected when Sco X-1 was in an active state, in ~20 minute dips between flares and prior to a transition to an extended quiescent state; in these cases QPO frequency varied between 10 and 20 Hz and was strongly correlated with source intensity. The transition between an active and a quiescent state was marked by variations in QPO frequency between 6 and 16 Hz which occurred on time scales of several minutes, with no intensity correlation. When the source finally entered an extended quiescent state, the QPO frequency settled down in the 6–8 Hz range and was slightly anticorrelated with intensity, confirming the relation for the quiescent state previously reported by Middleditch and Priedhorsky. We also find quiescent intervals when the 6 Hz QPO disappear. These results suggest that the QPO are associated with the transition between the two source states. The data also show that the intensity-dependent low-frequency noise has a power typically less than 10% of the power in the QPO when they are present but becomes stronger as the source intensity increases and the QPO disappear; this is the opposite to the case of GX 5−1.

We search for a correlation between the QPO modes and the spectral properties of the source using the two-component blackbody plus unsaturated Compton spectral model proposed in 1985 by White, Peacock, and Taylor. A correlation between QPO frequency and blackbody luminosity is found that is independent of the intensity state of the source. These results are discussed in terms of previously proposed models. We also present an oscillating thick disc obscuration model to explain the observed QPO and X-ray spectral behavior from Sco X-1.

Subject headings: stars: individual (Sco X-1) — stars: pulsation — X-rays: binaries

I. INTRODUCTION

Quasi-periodic oscillations (QPO) with frequencies between 20 and 40 Hz and amplitudes of up to 6% were recently discovered from the bright galactic bulge source GX 5−1 (van der Klis *et al.* 1985*a*). In GX 5−1 the QPO frequency shows a strong positive correlation with source intensity. The QPO are most coherent when the intensity is lowest, and both QPO and low-frequency noise (LFN) decrease in strength at the highest intensity levels. The oscillations cannot directly reflect the underlying rotation period of a compact object, and their interpretation is open to a number of possibilities (see van der Klis *et al.* 1985*a*).

Some proposed models involve a neutron star with a magnetic field strong enough to form a small magnetosphere (~10^9 G). In the beat-frequency model (BFM), proposed by Alpar and Shaham (1985) and further developed in Lamb *et al.* (1985), the QPO are interpreted as a modulation of the mass-accretion rate at the difference frequency between the Keplerian frequency of matter circulating at the inner edge of an accretion disk, and the neutron star magnetosphere. Other versions of the BFM were proposed by Morfill and Trümper (1985) and by Berman and Stollman (1986). These models have been influenced, in part, by the recent discovery of binary millisecond radio pulsars which may be the remnants of bright galactic bulge sources; the field strengths inferred from the pulsar spin-down gives values of ~10^9 G (cf. van den Heuvel, van Paradijs, and Taam 1986).

Two models for the QPO have been considered in some detail which do not require the neutron star to have a significant magnetosphere, such that the accretion disk "touches" the neutron star surface. Hameury, King, and Lasota (1985) in an adaptation of King's (1985) model for dwarf nova oscillations, identify the observed frequency with the rotation rate of a strongly differentially rotating boundary layer between accretion disk and neutron star surface. In another model proposed by Boyle, Fabian, and Guilbert (1986), oscillations in an accretion disk corona are invoked to explain the QPO.

Quasi-periodic oscillations similar to those from GX 5−1 have now been discovered from Sco X-1 (Middleditch and Priedhorsky 1985, 1986, hereafter MP85 and MP86), Cyg X-2

[1] On leave from I.C.R.A., Department of Physics "G. Marconi," University of Rome.

(Hasinger *et al.* 1986), GX 349+2 (Lewin *et al.* 1985), GX 17+2 (Stella, Parmar, and White 1985), 4U 1820−30 (Stella, White, and Priedhorsky 1985), and GX 3+1 (Lewin *et al.* 1986). The wide variety of QPO properties which has recently been found from the Rapid Burster (MXB 1730−335; Stella *et al.* 1985) shows that also the oscillations from this source, discovered by Tawara *et al.* (1982), fall in the same category. A forgotten first glimpse of the QPO from Sco X-1 may have been the report by Angel, Kestenbaum, and Novick (1971).

The 2–10 keV variability of Sco X-1 is characterized on a time scale of hours to days by a succession of quiescent states with relatively little variability, and active states containing episodes when the source flares by a factor of 2 or more on a time scale of minutes (cf. Canizares *et al.* 1973). During the flares the X-ray spectrum hardens considerably (White *et al.* 1976). Both the flaring and quiescent intervals can last many (typically 12) hours. The flaring episodes can be interrupted by short, 20–30 minute dips during which the intensity drops to about the quiescent level; these are of particular interest for the present analysis.

In this paper we present the results of a study of QPO in *EXOSAT* observations of Sco X-1 made in 1983 August and 1984 March. This study was prompted by the discovery of QPO in the quiescent state of Sco X-1 (MP85*a*) and led to the first report of QPO in the active state and during the transition to quiescence (van der Klis *et al.* 1985*b*, hereafter K85; and van der Klis and Jansen 1985*a*, *b*, hereafter KJ85*a*, *b*). Following these early reports further work showed that the important differences between the QPO first reported in MP85 and those first reported in K85 coincided with two different intensity/spectral states of the source in the two cases (van der Klis 1985; Middleditch 1985). Further work reported by Priedhorsky (1985) and Priedhorsky *et al.* (1986, hereafter P86) showed the existence of a strict correlation between the QPO and hardness ratio mode. After giving the observational details in § II, we discuss the properties of the QPO and their dependence on the overall state of the source in § III. In § IV we report on the spectral dependence of the QPO in terms of a two component spectral model. The consequences of these results for magnetic and nonmagnetic neutron star models are discussed in § V, and our conclusions are summarized in § VI.

II. OBSERVATIONS

We will report on a ∼20 hr *EXOSAT* observation of Sco X-1 obtained on 1983 August 29 and 30 and a series of three shorter ∼5 hr observations made on 1984 March 11, 12, and 13. The observational details are summarized in Table 1. The data were obtained with an array of eight ∼200 cm^2 proportional counter detectors in the medium energy (ME) instrument (Turner, Smith, and Zimmermann 1981). Each detector is multilayered consisting of an argon-filled (Ar) chamber sensitive in the 1–15 keV energy band over a xenon-filled (Xe) chamber sensitive in the 5–35 keV band. Four of these detectors were pointed directly at the source, but, because of dangerously high count rates in argon, only the Xe chambers were switched on. Four similar detectors were partially offset such that the source was at 5%–10% of the collimator response. In the offset detectors both the Ar and Xe chambers were operated.

Accumulations were obtained with a time resolution of about 8 ms (1/128 s) from the summed output of all eight Xe detectors during the first 12.5 hr of the 1983 August observation and the entire 1984 March 11 observation. For the 1984 March 12 and 13 observations, 8 ms data were obtained from the four offset Ar chambers. The 8 ms data are continuous with a nearly constant dead-time loss of ∼1% (approximately independent of source count rate). The raw count rate over the whole Xe detector array varied between 1600 and 5700 counts s^{-1} and includes an approximately constant background of ∼580 counts s^{-1}.

For the 1983 August observation, accumulations were also obtained with 31.25 ms resolution from both the four Xe chambers pointed directly at Sco X-1 and independently from the summed signal of the four partially offset detectors. The latter data thus contain both Ar and Xe counts, in a ratio of about 3:1. The 31.25 ms data are affected by electronic and data-handling dead-time losses varying between 30% and 60% and show dead-time corrected count rates per four detectors between 1200 and 4900 counts s^{-1} in Xe and 1100 and 3100 counts s^{-1} in Ar. These numbers include background levels of roughly 290 counts s^{-1} (Xe) and 36 counts s^{-1} (Ar).

The spacecraft pointing direction was changed slightly on two occasions during the 1983 August observation. This resulted in small changes in the collimator efficiencies. Count rates quoted in Tables 2–4, Figures 2–5, and throughout the text are background-subtracted and are corrected for dead time and to 100% collimator efficiency over four detectors (an array half).

Sco X-1 was also simultaneously observed with a gas scintillation proportional counter (GSPC: Peacock *et al.* 1982). Different gain settings were used at different times to allow spectral measurements in the 2–15, 2–30 or 2–60 keV ranges. Spectral data were also available from the ME. However, these data show subtle differences when compared to the simultaneous GSPC results, with an excess of counts above 10 keV. We attribute this to the extreme collimator angles at which the Ar detectors were operated which caused increased transmission of high-energy photons. Because of this, the ME spectra have been ignored for the present analysis.

The GSPC data have been previously discussed in White, Peacock and Taylor (1985, hereafter WPT). The GSPC light curve given by WPT indicates that the source was in an active state from the start of the 1983 observation until ∼09:00 UT on August 30 when it began an extended quiescent interval.

TABLE 1

OBSERVATION LOG

Date	Time (UT)	8 ms Data	31.25 ms Data	Spectral State	QPO
1983 Aug 29.....	23:08–11:30	Xe	Xe and Ar	Active	10–20 Hz
	11:30–18:44	no	Xe and Ar	Quiescent	6–8 Hz
1984 Mar 11.....	2:05–7:37	Xe	no	Active	10–20 Hz
1984 Mar 12.....	3:30–8:22	Ar	no	Quiescent	Not seen
1984 Mar 13.....	0:59–4:35	Ar	no	Quiescent	Not seen

The quiescent state lasted at least until the end of the GSPC observation at 19:30 UT. The X-ray light curve obtained from the 31.25 ms Xe data in a somewhat higher energy band is identical to this with the exception that the amplitude of the flaring is larger. This might be expected since the flares in Sco X-1 are known to be hard (White *et al.* 1976).

III. RESULTS

a) Quasi-periodic Oscillations

The analysis of the high time resolution data follows the approach taken by van der Klis *et al.* (1985*a*). The 8 ms data were divided into 64 s blocks, each containing 8192 flux samples, and the 31.25 ms data into 128 s blocks, each containing 4096 samples. A power spectrum was calculated from each block of data using a fast Fourier transform. These power spectra were then assembled into a two-dimensional (t, ν) diagram in which the power measured at time t at a particular frequency ν is indicated by black and white regions (Figs. 1*a* and 1*b*).

It was immediately evident from the (t, ν) diagram (Fig. 1*a*), constructed from the 8 ms data of 1983 August, that 10–20 Hz QPO were detected in the active state during short ($\sim$20 minute) dips in the intensity and during the transition to the quiescent state (K85, KJ85*a*, *b*). This result was later confirmed by P86 and by Pollock *et al.* (1986); a broad band of power between 14 and 24 Hz was noted by MP86. The 31.25 ms Xe data (Fig. 1*b*) showed QPO between 6 and 8 Hz similar to those first reported by MP85, 86 during a different quiescent state. During this interval the 8 ms data were not available. In the 31.25 ms data mode, the 10–20 Hz QPO detected during the active state straddle the 16 Hz Nyquist frequency. Between 12:05 and 12:50 UT a transition from $\sim$15 Hz to $\sim$6 Hz QPO occurs. A sequence of four power spectra is shown in Figure 2 to illustrate the evolution of the QPO during one of the dips in the active state. The broad QPO peak appears and disappears as the intensity passes through a minimum with, in addition, the broad peak shifting to a lower frequency as the intensity drops.

The centroid frequency of the peaks (hereafter QPO frequency) and their width and strength were measured by fitting a Lorentz function to the individual power spectra obtained from one data block of 64 or 128 s. Over the entire data set the QPO frequency varies between 6 and 20 Hz, and the peak FWHM between 2 and 12 Hz. The power in the oscillations ranges up to values corresponding to 10% rms variation in the 5–35 keV source flux.

The data set was divided into three intervals designated *active* (23:08–10:07 UT), *intermediate* (10:07–12:50 UT), and *quiescent* (12:50–18:44 UT). The properties of the power spectra were determined in the active state and in quiescence as a function of intensity by sorting the spectra according to count rate (see van der Klis *et al.* 1985*a*). In the intermediate interval the individual power spectra were sorted into contiguous time bins. For Xe count rates exceeding 1300–1350 counts s^{-1} the peaks in the power spectra sometimes become very wide and tend to merge in the background noise, making them difficult to measure. Consequently, systematic errors may affect some of the values quoted for power spectra in this intensity range. The results from the 1983 observation are given in Tables 2, 3, and 4.

In the active state, QPO were only seen during the short dips and during the transition to the intermediate state. Until 10:07 UT on August 30, the QPO frequency ν was approximately linearly related to the 5–35 keV count rate I, with the same I, ν relation applying to each of the data segments (Fig. 3*a*). Unfortunately between 10:18 and 10:39 on August 30 the spacecraft pointing direction was being changed to a slightly different direction, and we cannot rule out that the corrected source flux was being affected by this. QPO were always detected during the interval 10:07–10:39 UT. Initially the QPO frequency drops from $\sim$15 Hz to $\sim$6 Hz within 6 minutes and then rises back to $\sim$10 Hz. After 10:39 UT when the spacecraft pointing was again stable, it is evident that the I, ν correlation found before 10:07 UT is replaced by a more complex variation. During the 50 minute interval until the end of the 8 ms data at 11:30 UT, the I, ν relation as measured from the power spectra with 8 ms resolution executes a loop (Fig. 3*b*). Average power spectra constructed from seven contiguous data segments illustrate this behavior (Fig. 4). Note that at all QPO frequencies the peaks are narrow: the data cannot be explained as "mode shifting" between two single different frequencies (e.g., 6 and 16 Hz).

After 11:30 UT, only data with 31.25 ms time resolution were available. Up until 12:05 UT, QPO were not detected below the 16 Hz Nyquist frequency. It is possible that higher frequency QPO were still present in this interval. Between 12:05 and 12:50 UT, the QPO frequency shows a final decrease from 16 Hz to 6 Hz that is not correlated to any change in intensity. As in the case of MP86 and P86, the transition is not sudden; all intermediate QPO frequencies occur. The interval between 10:07 and 12:50 UT, which is characterized by erratic fluctuations in QPO frequency on time scales from minutes to tens of minutes, is the one that we have defined as the "intermediate state." After 12:50 UT (with the source well into quiescence), strong 6–8 Hz QPO were detected until 16:05 UT. During this interval the count rate and QPO frequency showed an *anti*-correlated behavior (Fig. 3*c*) similar to that reported by MP86.

After 16:05 UT, QPO at frequencies below 16 Hz were weak and at times not detected. In particular, no QPO were detected from 17:10 UT until the end of the ME observation at 18:44 UT (their rms amplitude was at least a factor of 2 below the typical value seen earlier). The disappearance of the QPO around 17:00 UT may be related to a gradual rise in count rate through quiescence—the QPO disappeared when the Xe count rate exceeded $\sim$1500 counts s^{-1}.

During the 1984 March 11 observation the source was in an active state. Strong ($\sim$10%) QPO with frequencies of 13–20 Hz were detected at the beginning and end of the observation when the source was relatively quiet. The I, ν relation was consistent with the one observed during the active state in 1983 August. During the final hour of the observation the source became quiescent, but another intermediate state (as defined by an erratic I, ν relation) was not observed.

Throughout the observations on 1984 March 12 and 13, the source was quiescent. Data obtained from the (1–15 keV) Ar detectors with a time resolution of 8 ms do not show QPO with an upper limit of $\sim$1%.

b) Low-Frequency Noise

In this section we describe the properties of the low-frequency noise (LFN), which we define as the variability component that dominates the power spectra at the lowest observed frequencies and whose power decreases monotonically as a function of frequency. This LFN was found in all

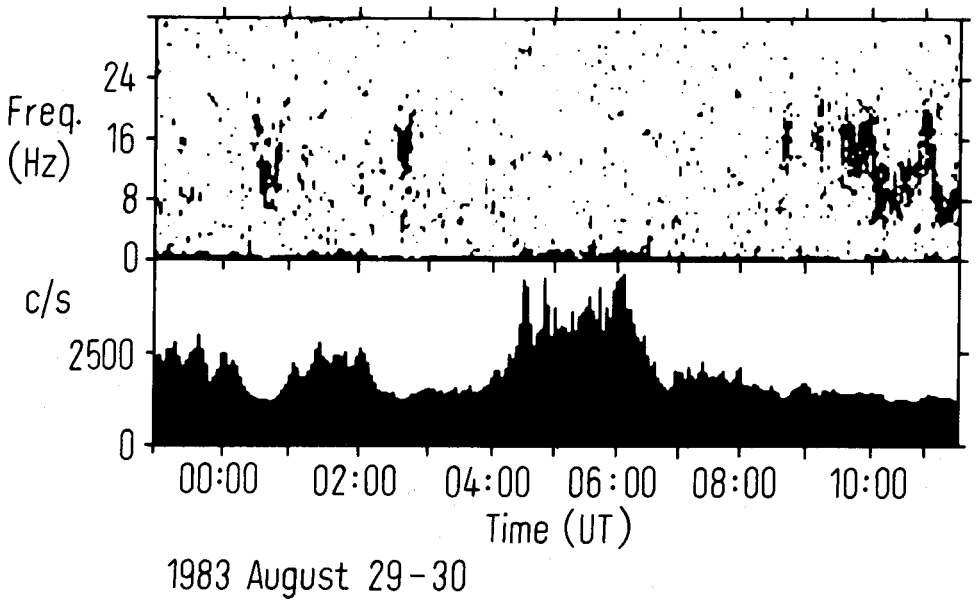

FIG. 1*a*

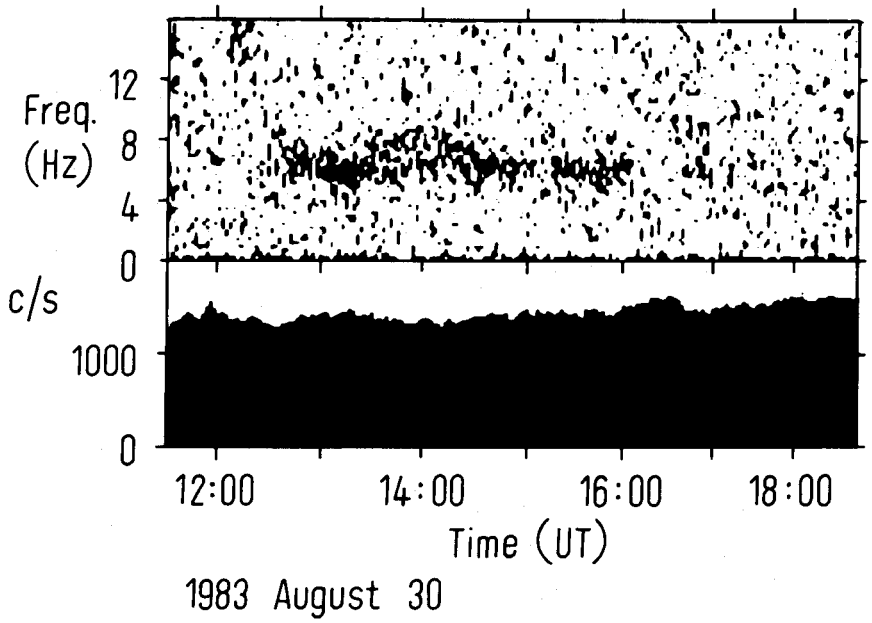

FIG. 1*b*

FIG. 1.—(*a*) The time-frequency diagram (*upper*) and the simultaneous 5–35 keV count rate (*lower*) during the 1983 August observation as obtained from 8 ms resolution data. The black points in the upper diagram indicate that a high power density was measured at the corresponding frequency (*left-hand scale*) and time (*lower scale*). The spectra have been smoothed with a 0.75 Hz wide rectangular window. QPO are clearly seen during interflare dips and near the end of the observation during the initial stages of the transition to quiescence. Note the rapid variations in QPO frequency in the latter interval. (*b*) As (*a*) but for the 31.25 ms resolution data. The spectra have been smoothed with a 0.44 Hz wide rectangular window. Note the rapid transition of QPO frequency from the 16 Hz Nyquist frequency down to ~6 Hz near 12:30 UT. Thereafter the QPO settle in a nearly constant 6 Hz mode, interrupted only by a short 8 Hz interval near 14:00 UT for the lowest observed posttransition intensity, until 16:00–17:00 UT when QPO disappear.

power spectra, but, as reported previously (KJ85*a*, *b*, MP86), it was weak, and in most cases it was only detected below 1 Hz. The slope of the LFN was measured by including a power-law component in the function which was fitted to the power spectra. It was generally found to be in the range 1.4–2, with a tendency toward steeper LFN during flaring episodes. In some cases, notably at the peak of flares, the slope exceeds 2, indicating it to be too steep for the parameters of the LFN to be reliably estimated from a Fourier transform (Deeter 1984). The weakness of the LFN when QPO were present prevents a reliable estimate of the LFN strength from the fit parameters. We estimated the strength of the LFN by directly summing up the excess power in the range 1/64–1 Hz, and the results are given in Tables 2, 3, and 4 and in Figures 5*a* and 5*c*. The power in the LFN was always less than ~20% of the power in the QPO and rarely exceeded 10% of it.

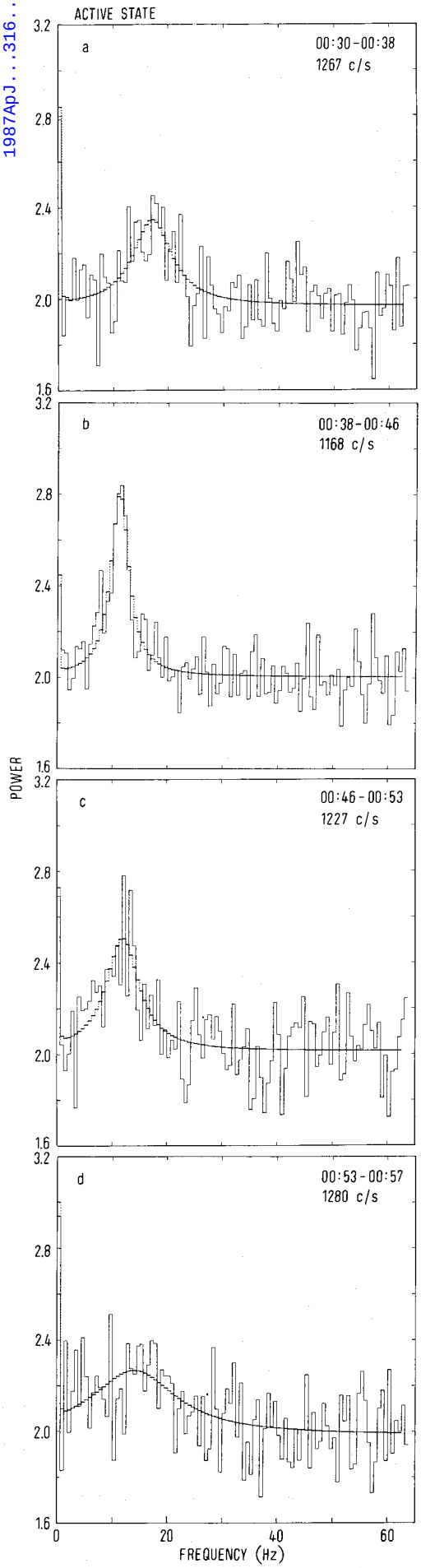

FIG. 2.—The evolution of the QPO peak during one of the interflare dips. Average 5–35 keV count rate and the time interval (UT) corresponding to each power spectrum are indicated. Note how the peak narrows then flattens back out on a time scale of minutes, and how its centroid frequency shifts to lower values when the flux drops.

TABLE 2

BEST-FIT PARAMETERS OF POWER SPECTRA: ACTIVE STATE

I^a (counts s^{-1})	N^b	ν^c (Hz)	FWHM[d] (Hz)	Relative QPO Strength (% rms)	Relative LFN Strength (1/64–1 Hz) (% rms)
1174.....	11	11.0 ± 0.3	6.2 ± 0.6	8.0 ± 0.3	1.7 ± 0.2
1217.....	16	14.2 ± 0.2	6.0 ± 0.5	8.8 ± 0.2	1.7 ± 0.2
1249.....	28	14.9 ± 0.2	7.3 ± 0.5	8.7 ± 0.2	1.5 ± 0.2
1287.....	16	16.4 ± 0.3	9.2 ± 0.7	9.2 ± 0.5	1.7 ± 0.2
1323.....	9	16.9 ± 0.5	8.9 ± 1.1	8.0 ± 0.4	2.6 ± 0.2
1366.....	4	20.7 ± 0.5	1.6 ± 1.1	5.2 ± 0.5	2.2 ± 0.3
1400.....	6	14.4 ± 2.3	20.2 ± 4.4	7.6 ± 0.6	1.9 ± 0.3
1437.....	4	22.0 ± 2.5	32.3 ± 5.4	10.4 ± 0.7	1.5 ± 0.4

NOTE.—Errors are projection of the $\chi^2 + 1$ contours on coordinate axes in parameter space.
[a] 5–35 keV count rate.
[b] Number of power spectra.
[c] QPO frequency.
[d] Full width at half-maximum of QPO peak.

TABLE 3

BEST-FIT PARAMETERS OF POWER SPECTRA: INTERMEDIATE STATE

t_{lim} (UT)	I (counts s^{-1})	N	ν (Hz)	FWHM (Hz)	Relative QPO Strength (% rms)	Relative LFN Strength (1/64–1 Hz) (% rms)
10:39 10:54 }	1174	14	10.9 ± 0.4	6.8 ± 0.9	8.1 ± 0.4	1.2 ± 0.4
10:58 11:02 }	1232	4	17.7 ± 0.6	6.3 ± 1.4	8.6 ± 0.6	1.5 ± 0.6
11:04 11:10 }	1316	4	16.6 ± 0.4	5.7 ± 1.0	8.4 ± 0.5	2.2 ± 0.3
11:23 11:27 }	1321	1	13.2 ± 0.6	4.8 ± 1.7	9.8 ± 0.8	2.7 ± 0.6
	1295	5	8.9 ± 0.3	3.5 ± 0.8	8.2 ± 0.4	2.1 ± 0.3
	1242	13	6.9 ± 0.2	3.5 ± 0.5	6.6 ± 0.3	1.3 ± 0.4
	1178	4	9.7 ± 0.8	7.1 ± 1.5	8.0 ± 0.7	1.4 ± 0.6

TABLE 4

BEST-FIT PARAMETERS OF POWER SPECTRA: QUIESCENT STATE

I (counts s^{-1})	N	ν (Hz)	FWHM (Hz)	Relative QPO Strength (% rms)	Relative LFN Strength (1/64–1 Hz) (% rms)
1236.....	6	7.92 ± 0.26	1.3 ± 0.7	6.59 ± 0.15	1.80 ± 0.35
1280.....	9	6.27 ± 0.11	1.0 ± 0.4	4.22 ± 0.20	1.86 ± 0.29
1323.....	18	6.14 ± 0.10	1.6 ± 0.3	4.77 ± 0.23	1.54 ± 0.20
1366.....	27	6.07 ± 0.07	1.4 ± 0.2	4.47 ± 0.18	2.03 ± 0.14
1411.....	23	6.05 ± 0.10	1.7 ± 0.3	4.8 ± 0.4	1.83 ± 0.16
1456.....	14	6.0 ± 0.4	3.2 ± 1.2	4.2 ± 0.4	1.82 ± 0.21
1501.....	6	5.93 ± 0.26	2.0 ± 1.1	4.7 ± 1.0	2.13 ± 0.40

We estimated the LFN strength in the flaring episodes (when no QPO were detected), from the fit parameters using intensity-sorted power spectra. The LFN power is found to rise considerably with intensity and finally, in terms of fractional rms variation, approaches the strength of the QPO seen in the interflare dips (Fig. 5*b*).

During the March 11 observation, when the source was active and strong QPO were observed, the LFN was weak (<1% rms). However, the March 12 and 13 data, taken in the 1–15 keV band when the source was quiescent but did not show significant QPO, show LFN with a strength corresponding to a ~2.5% rms flux variation (0–16 Hz). The statistics of these data are very good (3000–3500 counts s^{-1} with very small dead time), and significant LFN excess power is detected up to ~25 Hz.

During the quiescent part of the 1983 August observation we were able to simultaneously measure the strength of the QPO/LFN separately in the Ar and Xe detectors from the 31.25 ms data. We confirm the finding of P86, that the QPO have a harder spectrum than the average source flux: the rms fractional variation in the intensity caused by the QPO is 1.8% ± 0.2% in Ar (1–15 keV) and 4.6% ± 0.2% in Xe (5–35 keV). For the LFN (1/64–1 Hz) these values are <1% (2 σ) and 1.9% ± 0.2%, respectively. These numbers were corrected for

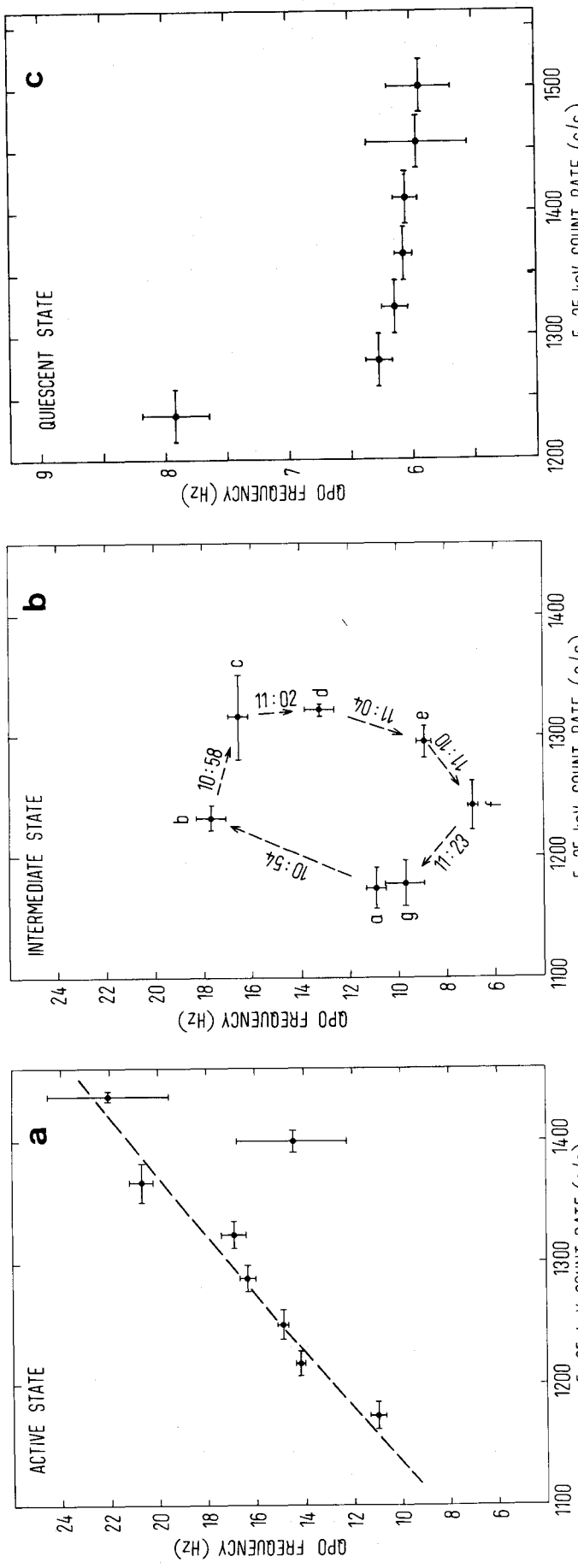

FIG. 3.—The dependence of QPO frequency on count rate during (*a*) the low flux episodes in the active state, (*b*) the intermediate state, and (*c*) quiescence. (*a*) and (*c*) were obtained by intensity sorting (see text); (*b*) was obtained from time-consecutive power spectra. The time order and limiting times of each power spectrum are indicated in (*b*).

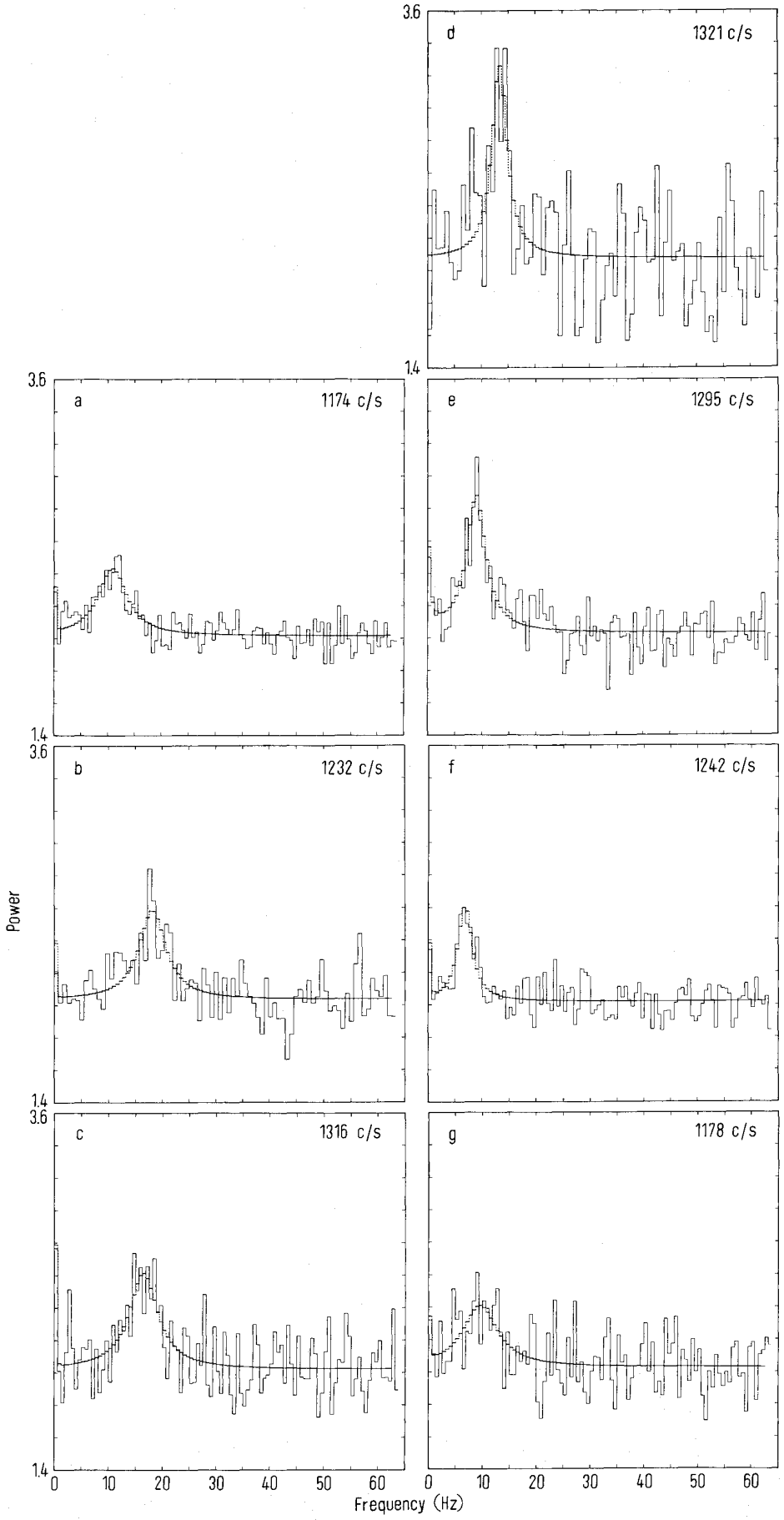

FIG. 4.—Time evolution of the power spectra in the intermediate state. This is the data on which Fig. 3*b* is based. Note that the peaks are well defined at all frequencies between 6 and 18 Hz occurring in the loop.

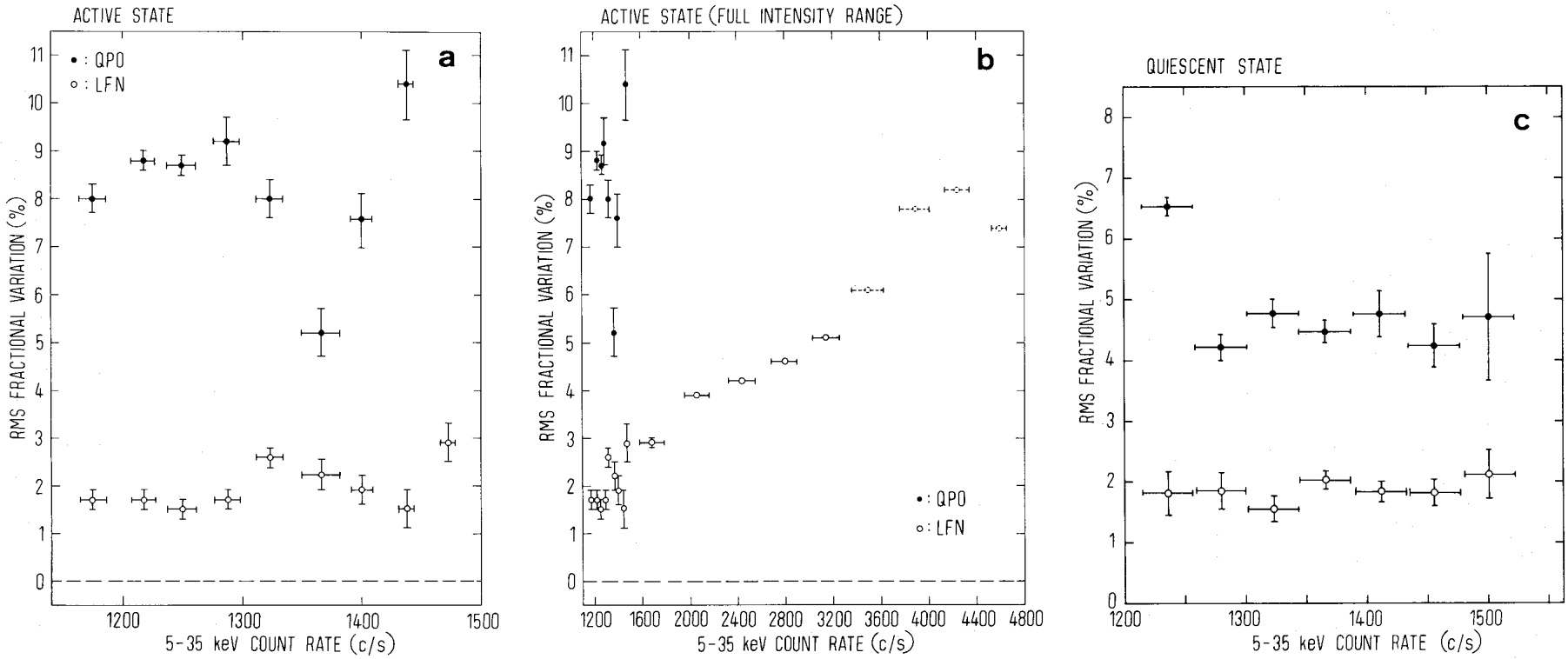

FIG. 5.—The dependence on count rate of QPO (*filled circles*) and LFN (*open circles*) strength, expressed in terms of the rms fractional variation in the 5–35 keV source flux, during (*a*) the low flux episodes in the active state, (*b*) the flaring episodes, and (*c*) quiescence. Note that the LFN is always considerably weaker than the QPO and that only in strong flares does it approach the level (in terms of fractional variation) of the QPO when they are present. In (*a*) and (*c*) the LFN was too weak to be reliably measured by fitting a function to the power spectrum. Instead, the excess power between 1/64 and 1 Hz was directly summed up. The QPO strength, and in (*b*) also the LFN strength, were calculated from fits to the power spectra. Dashed points in (*b*) correspond to cases, where the power-law slope of the LFN was close to, or exceeded, 2. Only the data in (*c*) were affected by appreciable dead time and have undergone a dead-time correction.

first-order dead-time effects, taking into account the effects of channel cross-talk; we assumed that both the QPO and LFN differ between the two channels only in amplitude.

IV. A RELATION BETWEEN QPO PROPERTIES AND X-RAY SPECTRUM

The continuum spectrum of Sco X-1 can be well described by a two-component model consisting of a blackbody and an unsaturated Comptonized spectrum with the latter approximated by the function $E^{-\Gamma} \exp(-E/kT)$ (WPT). In this model the flaring intervals are caused primarily by increases in the luminosity of the blackbody component from 10% to 40% of the total. The derived radius of this component (assuming a distance of 1.5 kpc; WPT) varies between 2 and 6 km, suggesting that it is associated with the heated surface of (part of) a neutron star (WPT). White *et al.* (1986) show that this two-component model provides a better representation of the data on several bright low-mass X-ray binaries than the earlier proposed self-Comptonized thermal bremsstrahlung model (Lamb and Sanford 1979) or the two-component model of Mitsuda *et al.* (1985).

The GSPC data from the observations reported here have

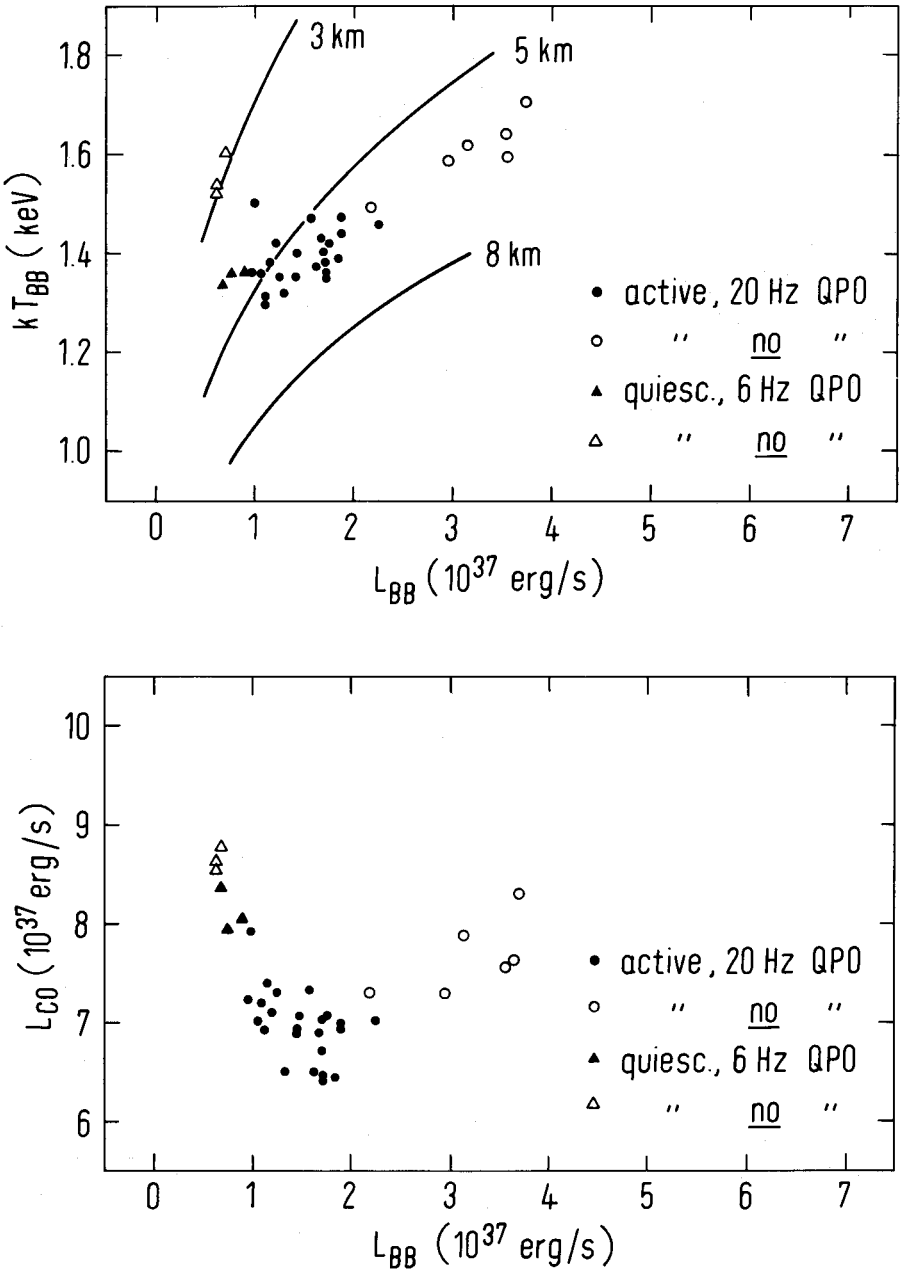

FIG. 6.—Spectral correlations of the QPO. The blackbody temperature and the luminosity of the Comptonized component are plotted separately as functions of the blackbody luminosity. Filled symbols indicate the presence of QPO; open symbols indicate their absence. Note how on both branches the QPO become undetectable when the luminosity exceeds a certain level. The spectral parameters in the intermediate state were indistinguishable from those in the active state and were also plotted as filled circles.

already been discussed by WPT with particular emphasis on the properties of the iron K line at 6.7 keV. We have reanalyzed the GSPC spectral data taken during these observations in order to investigate the relationship between the QPO properties and the spectral state of the source. This reanalysis concentrated on (1) the interflare dips in the active state and the transition to the intermediate state when the 10–20 Hz QPO appear, (2) the intermediate state, and (3) the quiescent state when the 6–8 Hz oscillations were strong.

Figure 6 summarizes the observed variations in some of the spectral parameters. The overall results are similar to those given by WPT. Active and quiescent states form two branches in the diagrams, with increases in the luminosity and temperature of the blackbody component explaining the hard flaring. In quiescence the blackbody temperature increases with source intensity, but its radius shrinks and this causes its luminosity to remain constant or decrease slightly. The luminosity of the Comptonized component increases with intensity in quiescence. Spectra taken during intervals when QPO were detected are indicated in Figure 6 by filled symbols; intervals when QPO are not detected are indicated by open symbols. Clearly QPO were mainly observed near the branching point between the quiescent and active state.

The spectral changes seen when QPO are present are very small when compared to the major changes seen when the source is flaring. In quiescence the equivalent hydrogen column density N_H to Sco X-1 obtained from the fitting procedure has very large error bars and is strongly correlated with the luminosity of the blackbody component and Γ. If an N_H of zero is assumed, then the luminosity of the blackbody component is close to zero (it is no longer statistically required) and the best fit value for Γ is ~ 0.8. However, an independent measure of N_H from simultaneous objective grating measurements using the *EXOSAT* low-energy telescopes (Brinkman *et al.* 1985) constrains N_H to $\gtrsim 2 \times 10^{21}$ H cm^{-2}. This constraint results in a finite blackbody luminosity of $\sim 1 \times 10^{37}$ ergs s^{-1} and Γ in the range 1.2–1.3. Nonetheless, we are dealing with very strong interdependence of the parameters, and any interpretation must be treated cautiously.

In spite of these problems it is notable that when we plot the frequency of the QPO against blackbody luminosity,[2] L_{BB}, there is a strong correlation between the two (Fig. 7). The looping behavior during the intermediate state and the anticorrelation between ν and I in quiescence are approximately matched by similar behavior of L_{BB} versus I so that the relation between ν and L_{BB} remains the same for active, interme-

[2] Note that the frequency-intensity relations in the active and quiescent states were derived by sorting the power spectra according to Xe count rate. This was not feasible for the GSPC X-ray spectra, so we first separately determined the relation between blackbody luminosity and Xe count rate and then applied this relation to the frequency measurements.

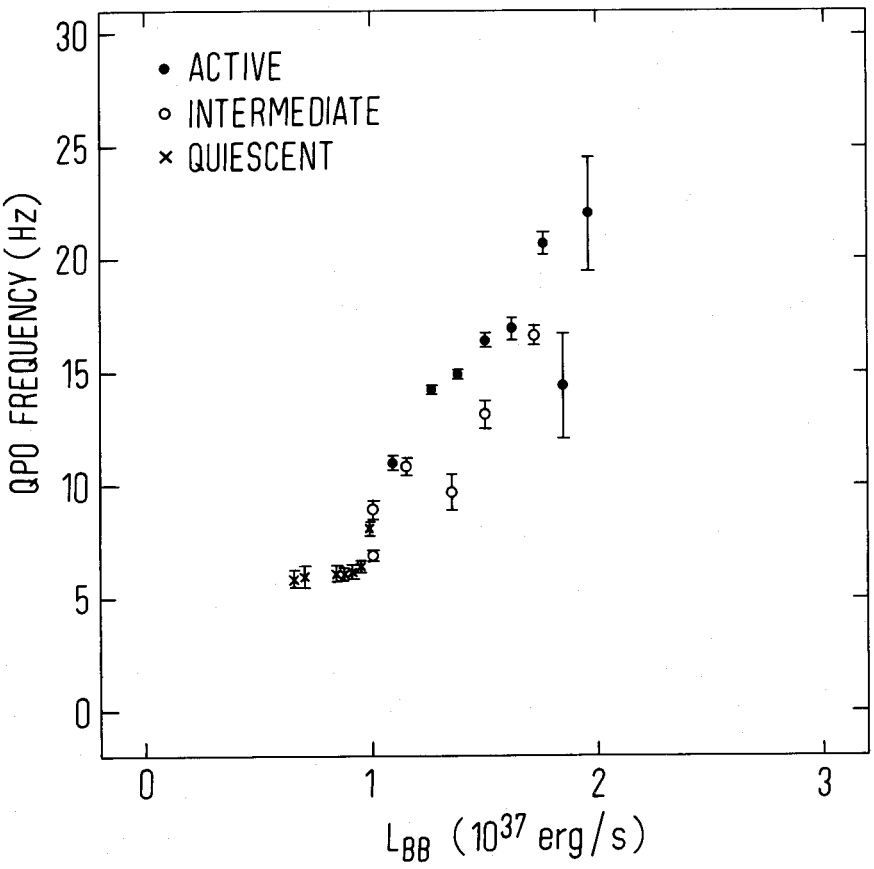

FIG. 7.—The dependence of QPO frequency in all three states on blackbody luminosity. Except for the intermediate state, frequency and blackbody luminosity were not measured strictly simultaneously, but were coupled via the 5–35 keV count rate. Although considerable systematic effects on the blackbody luminosities can not entirely be excluded (see text), a simple dependence with QPO frequency seems to exist.

diate, and quiescent states, even though the QPO are present only when the blackbody component is weak.

V. DISCUSSION

In the following, we first summarize the main observational results as obtained by us (K85; KJ85*a*, *b*; this paper) and other authors (MP85, 86; Pollock *et al.* 1986). We then compare these results with previously proposed models and finally we consider some aspects of an obscuring thick disk scenario as an explanation for the QPO, LFN, and spectral behavior.

a) Observational Summary

The properties of the QPO from Sco X-1 indicate the existence of four different fast timing modes which can be associated with the quiescent and active intensity states:

1. *The flaring episodes in the active state*, during which QPO are not detected and the LFN is strong (4%–8% rms in the 5–35 keV band). These episodes can be spectrally characterized by a strongly variable blackbody component.

2. *The low-intensity episodes in the active state* (including both interflare dips and the initial stages of transition to quiescence) where the 10–20 Hz QPO first reported in K85 are seen whose frequency is found to be strongly correlated with intensity (when the QPO peak is sufficiently narrow for the frequency to be measured).

3. *The "intermediate" state*, spectrally similar to the low-intensity episodes in the active state, but characterized by rapid (time scales as short as several minutes) variations in the QPO frequency between 6 and 20 Hz. During this interval, loops in the frequency-intensity relation are sometimes seen. We observed this intermediate-state behavior during a transition from an active to a quiescent state (KJ85*a*, *b*); Pollock *et al.* (1986) apparently observed it during the opposite transition and maybe even in the middle of a quiescent state. We note that looplike structures are also seen in dwarf nova oscillation frequency-intensity diagrams (e.g., Patterson 1981).

4. *The quiescent state*, during which the 6–8 Hz QPO first reported in MP85 and MP86 were detected. The QPO are seen only during the lowest 70% of the total intensity range. Their frequency is weakly anticorrelated with the source intensity. In this state, the blackbody component is very weak. Intensity changes are dominated by the variations in the Comptonized component. A different type of quiescent state is possibly seen on 1984 March 12 and 13 where in the 1–15 keV band no QPO are detected but relatively strong LFN is observed.

In general, QPO are detected when the spectral characteristics of the source approach the branching point between the two intensity states. The occurrence of a particular QPO/LFN state is observed to be strictly correlated with the spectral behavior. In addition a correlation was found between QPO frequency and blackbody luminosity which held for all states in which QPO were detected. The strength of the QPO in the 5–35 keV band was ~9% rms in the active and intermediate state and ~5% in quiescence. Simultaneously occurring LFN measured over the 1/64–1 Hz range was always much weaker than the QPO, typically 1%–2% rms.

b) Comparison with Proposed QPO Models

In comparing these data with proposed models, we first turn to magnetospheric models, in which the QPO are caused by the interaction of matter at the inner edge of a Keplerian accretion disk with a neutron star magnetosphere. Due to the compression of the magnetosphere the QPO increase in frequency when the accretion rate $\dot{M}$ increases.

The development of this class of models has been strongly influenced by the need to explain the strong dependence of QPO frequency on intensity observed from GX 5−1. To avoid the problem that the Keplerian frequency of matter circulating at the magnetospheric radius depends weakly on $\dot{M}$ (to the $\frac{3}{7}$th power) while the observed dependence in GX 5−1 is strong, the BFM was proposed (Alpar and Shaham 1985). In the BFM the QPO frequency ν arises as a beat between the Keplerian frequency ν_k and the neutron star rotation frequency ν_r; $\nu = \nu_k - \nu_r$. Several mechanisms are conceivable by which L_x could be modulated at this beat frequency; modulation of the accretion rate (Lamb *et al.* 1985; Berman and Stollman 1986), modulation of the disk emission (Morfill and Trümper 1985), or obscuration of the central source.

In each application of the BFM the observed relation between QPO frequency and intensity I can be used to predict a rotation rate and a magnetic field strength of the neutron star. This prediction is critically dependent on the conversion of I into $\dot{M}$ (*cf.* Lamb *et al.* 1985). If $\dot{M}$ is proportional to the total X-ray luminosity L_x, then from the L_x, ν relation we observe from Sco X-1 in the active state, the BFM predicts (for similar assumptions as in van der Klis *et al.* 1985*a*) a neutron star rotation period of roughly 4 ms, a magnetospheric radius r_m of ~35 km and (for a distance of 1.5 kpc) a magnetic field strength B_0 of $\sim 10^9$ G. By contrast, the raw I, ν relation predicts a longer rotation period of 10 ms and correspondingly different values for other parameters.

The anticorrelation between L_x and ν observed in quiescence might be expected from the BFM for low accretion rates when r_m exceeds the corotation radius. Accretion would in this situation be inhibited by centrifugal forces, but not necessarily over the whole magnetospheric boundary, such that some material might still accrete. However, L_x is not lower in quiescence than during the low-intensity episodes in the active state, as required in this interpretation. Also the L_x, ν relation actually observed in quiescence is different from the predicted one in that it does not pass through zero frequency and shows a sharp break near 1250 counts s^{-1} (Fig. 3*c*). Finally, the large rapid variations in QPO frequency with hardly any luminosity changes that are observed in the intermediate state also cannot be explained in a BFM where L_x is proportional to $\dot{M}$.

A better measure for $\dot{M}$ may be the blackbody luminosity L_{BB}, since this could be emission from the neutron star surface. The relation we observe in all states between QPO frequency and L_{BB} is approximately linear. It is less steep than when the total luminosity is considered, but it is still not flat enough to allow the identification of the QPO frequency with the Keplerian frequency of matter at r_m. The BFM applied directly to the L_{BB}, ν relation (Fig. 7) yields a neutron star spin period of roughly 30 ms, $r_m \approx 110$–130 km and $B_0 \approx 5 \times 10^9$ G. If the nonblackbody component originates outside the magnetosphere in the accretion disk, then this magnetospheric radius is too large to account for the fact that this component comprises up to 95% of the total X-ray luminosity.

To make any BFM work for Sco X-1 from the point of view of the correlation of the QPO properties with the X-ray spectrum, assumptions different from the preceding have to be made about the estimate of $\dot{M}$ from the X-ray intensity. As long as these assumptions are more or less arbitrary, it is not possible to exclude the simpler magnetospheric model where

the QPO frequency is identified with the Kepler frequency at the magnetospheric boundary.

Priedhorsky (1986) has recently pointed out that the rotational energy lost by a rapidly rotating weakly magnetized neutron star can be fed back into the disk (Ghosh and Lamb 1979) and may, during intervals of spin-down when the magnetospheric radius exceeds the corotation radius, play an important role in explaining the strength of the Comptonized component and the anticorrelation of its luminosity to L_{BB} in quiescence.

From the point of view of its *timing* properties, Sco X-1 presents two problems to beat-frequency models. The first is the absence of detectable coherent pulsations, which it shares with all QPO sources detected so far. This is a problem, because BFMs specifically require a rapidly rotating neutron star with a nonaxisymmetric magnetic field which in all proposed BFMs periodically interacts with the accreting matter. There are reasons why the pulsations might be weak (Lamb *et al.* 1985) but at some level they should be detected (MP86). For Sco X-1 MP86 have obtained an observational upper limit of 0.8% for the pulsed fraction of coherent pulsations below 250 Hz.

The second problem is the weakness of the low-frequency noise when QPO are present. With respect to this basic property of the power spectrum, Sco X-1 seems to be different from GX 5−1 and several other QPO sources. In GX 5−1, the power in the LFN (down to 0.5 Hz) and in the QPO is similar (van der Klis *et al.* 1985*a*), while in Sco X-1 we find that the power in the LFN even down to 1/64 Hz, is usually less than 10% of the power in the QPO. Moreover, the fact that the LFN becomes stronger when the QPO disappear suggests that the LFN is not directly related to the QPO in Sco X-1. Models (such as most BFMs) which require that the QPO are caused by "oscillating shots"—i.e., wave trains which give a positive net contribution to the total flux, explain the observed properties of GX 5−1 but fail to account for what is observed in Sco X-1 (unless one assumes a strong phase dependence between the oscillations in different shots; Lamb *et al.* 1985).

The two proposed nonmagnetospheric models (Hameury, King, and Lasota 1985; Boyle, Fabian, and Guilbert 1986) do not make quantitative predictions for the relation between QPO frequency and accretion rate.

c) *An Obscuration Model*

A model that has not, to date, received much attention is that in which the QPO are the result of quasi-periodic partial obscuration of the central source by, e.g., structure in the accretion disk. Simulated power spectra are shown in Figure 8 for two different obscuration geometries. Figure 8*a* shows the situation in which an obscuring straight edge is centered on a circular, uniformly emitting source. When the edge is quasi-periodically oscillating, a QPO peak is produced but no LFN. Figure 8*b* is the same situation as seen from a slightly different inclination, so that the edge is offset from the source center and the X-ray source is completely covered during half of each oscillation cycle. This leads to a power spectrum with QPO and appreciable LFN.

In the situation of Figure 8*a*, the QPO wave trains do *not* (as is the case in oscillating shot models) give a net contribution to the source flux but, rather, give equal positive and negative contributions which cancel, so that no LFN is produced. QPO–related LFN is produced in an obscuration model if the obscured region is not uniform. An extreme case obtains if during part of the oscillation cycle the X-ray emitting region becomes completely obscured (as in Fig. 8*b*) or completely uncovered. This results in a truncated (flat-topped or flat-bottomed) sinusoid wave train with an average level different from the nonoscillating flux. Thus, in an obscuration model the presence of QPO–related LFN is dependent on the detailed geometry of the obscuring medium and the emission region. The difference in the LFN between GX 5−1 and Sco X-1 can in such a model be due to the viewing geometry, i.e., *inclination*. The maximum LFN strength which can be produced by this mechanism is about equal to the strength of the QPO. The observed LFN might be stronger than this if there is additional non–QPO–related LFN.

Magnetospheric obscuration models in which periodic motion of obscuring matter at the magnetospheric boundary explains the QPO are conceivable (van der Klis *et al.* 1985*a*), but we will assume here that the neutron star does not have an appreciable magnetic field and that the disk can extend to the neutron star surface (see also Stella 1986). In the standard model (Shakura and Sunyaev 1973), for accretion rates approaching the Eddington limit, the inner radiation-pressure–dominated disk will have a half-thickness of ~ 30 km which decreases as $(1 - R^{-0.5})$, where R is the radius in neutron star radii. It has been proposed that the inner radiation-pressure–dominated regions of the accretion disk are unstable to thermal and secular instabilities and that the scale height will increase (see Pringle 1981 and references therein) until it becomes of the order of the radius r to the center. While its geometry is uncertain, it seems probable that such a thick disk may extend out to several hundred kilometers from the center. Without specifying the physics determining the exact shape and size of the inner thick disk, we will consider here whether such a geometry can explain the observed combination of fast timing and spectral behavior (see Fig. 9).

Nearly all gravitational energy will be released in the innermost part of the thick disk, close to the neutron star and at its surface. The resulting primary radiation will only be able to escape directly through a polar "channel" perpendicular to the disk plane (cf. Lamb *et al.* 1985). It will only be possible to observe the neutron star and the central disk region when we are looking close to pole-on. There are several ways in which radiation might be observed at higher inclinations: (1) the primary radiation can be scattered out of the polar channel; (2) if the thick disk is not completely optically thick radiation may be scattered through it; and (3) radiation might be reprocessed in the walls of the polar channel. If we identify the blackbody component in the spectrum of Sco X-1 with the emission from the neutron star surface and the Comptonized component with emission from the central disk regions and from the polar channel, then the flaring episodes can be interpreted as times when a decrease in h/r allows a more direct view of the central neutron star. The inclination of Sco X-1 is rather low (Crampton *et al.* 1976), which may be ideal for the occasional uncovering of the central region.

In such a thick disk geometry, the QPO could be caused by quasi-periodic oscillations in the thick inner accretion disk which partially obscures the radiation emitted in our direction out of the polar channel. The difference of our model with that of the Boyle, Fabian, and Guilbert (1986) is that the mechanism allowing the disk oscillations to modulate the source intensity is obscuration rather than reflection of X-rays. The combination of thick disk and viewing geometry would determine the radius vector of the point of interception of the line of sight and thereby the frequency of the QPO (see Fig. 9); the model requires that the thick disk is not optically thin. From

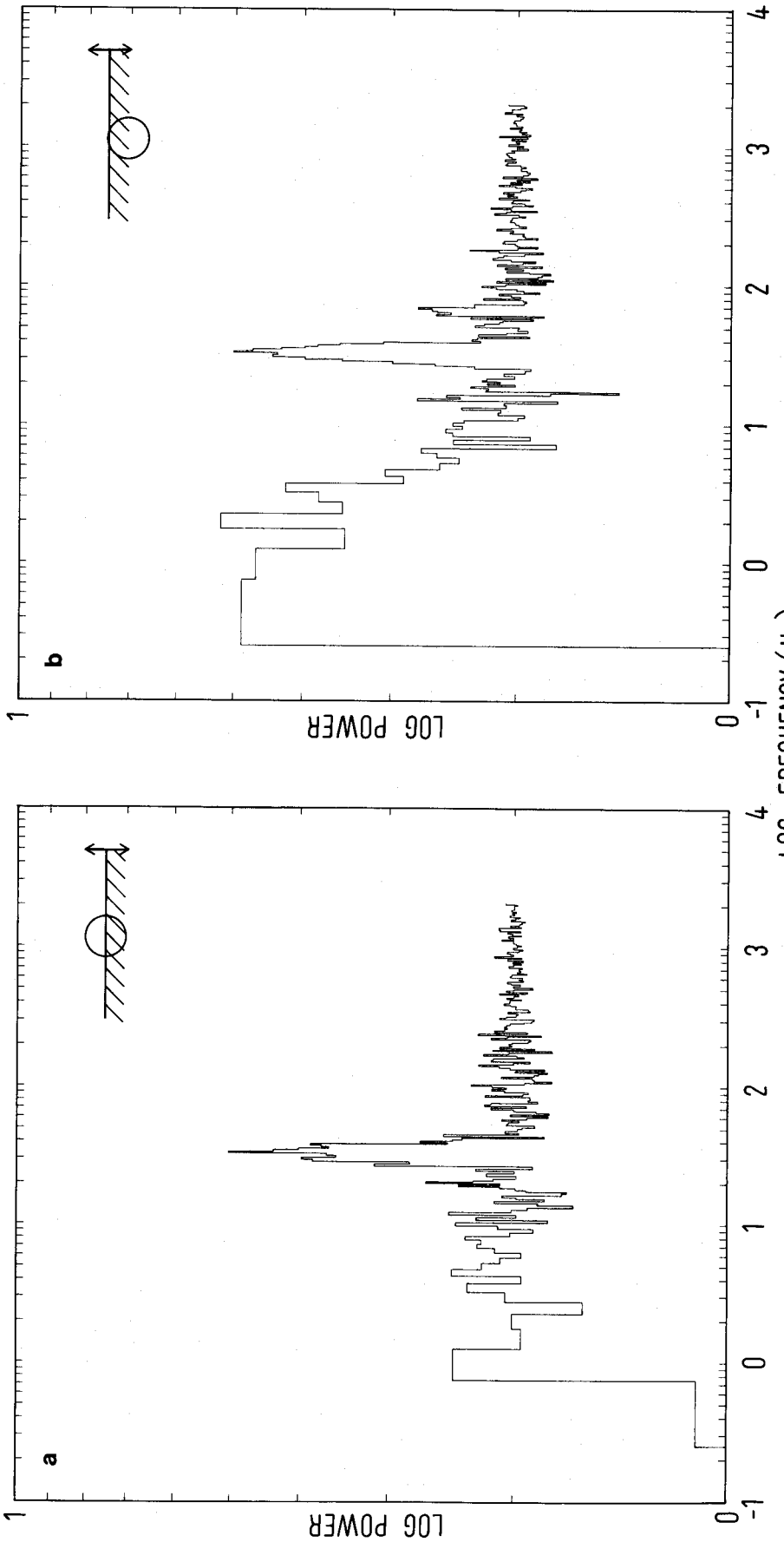

FIG. 8.—Simulated power spectra. A straight opaque edge oscillates quasi-periodically in front of a circular, uniformly emitting source. As indicated by the doodles in the upper right-hand corners of each frame, the equilibrium position of the edge was chosen (*a*) close to the center of the source and (*b*) close to its edge, respectively. A considerable change in the strength of the LFN is the consequence. The simulation may be considered as a highly idealized model for QPO caused by oscillations in an accretion disk, the difference between (*a*) and (*b*) being the inclination of the system. Note the appearance of the second harmonic in (*b*).

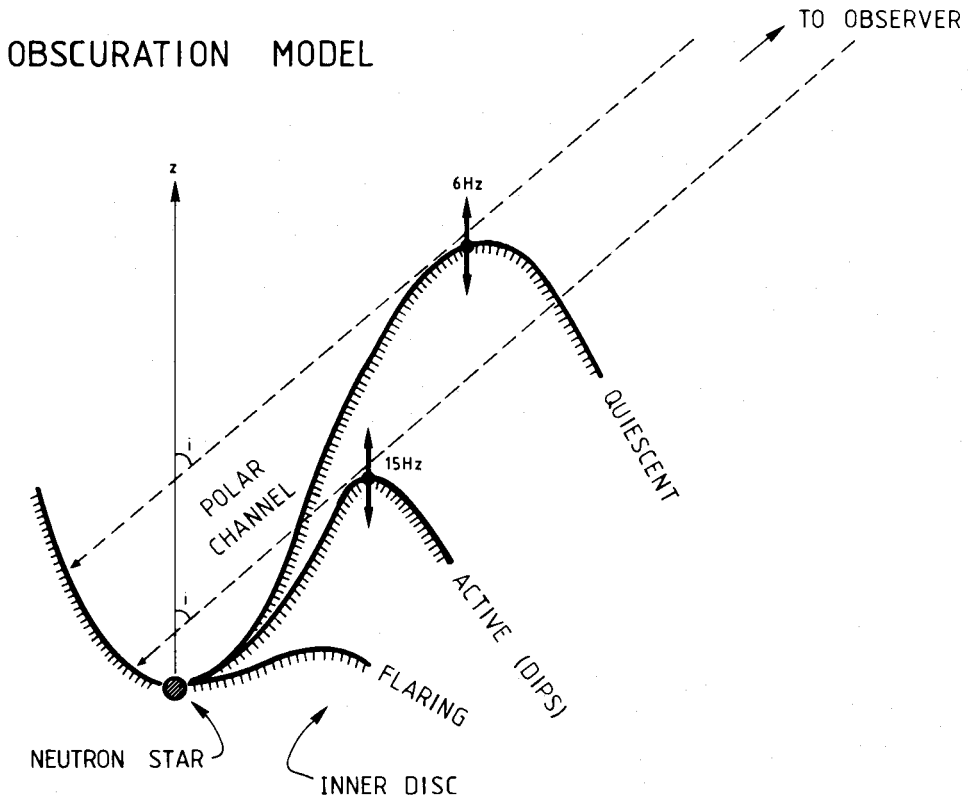

FIG. 9.—Schematic of a phenomenological oscillating thick disk obscuration model (see text). Thick dots indicate the interception point of the line of sight by the thick disk. The radius vector of this point determines the observable disk oscillation frequency. Radiation emitted out of the polar channel in our direction can be obscured for a wide range of inclinations. The source flares when the inner disk flattens out sufficiently to allow us a direct view of the neutron star.

simple considerations (e.g., Pringle 1981) one expects oscillations (or the passage of circulating blobs) in an accretion disk at radius r to occur at a frequency close to the Kepler frequency at r. The 6–8 Hz oscillations in quiescence would then indicate that the thick disk intercepts our line of sight at $r \sim 400$ km. In the low-flux episodes of the active state (10–20 Hz); this would be $r \approx 250$ km. During the flaring episodes finally, h/r becomes too small to obscure any appreciable emitting region, so that no QPO are produced. The amplitude of the QPO would tend to be larger when the source is close to transitioning from one state to the next and the disk rim is passing in front of the central source.

In this scenario the observed intensity variations are dominated by variations in the geometry rather than accretion rate. The smaller thick disk dimensions required in the active state imply a lower accretion rate than in quiescence; the uncovering of the central region compensates for the resulting lower X-ray production. The decrease in the blackbody luminosity associated with the transition to quiescence is suggestive of a progressive covering up of the central region, resulting in an X-ray spectrum dominated by the Comptonized polar channel emission.

If we identify the QPO frequency with the Kepler frequency at the outer boundary of the radiation-pressure–dominated region of the disk, we predict $\nu \propto \dot{M}^{-8/7}$ (Stella 1986). As in the case of the BFM, lack of exact knowledge of $\dot{M}$ precludes a direct comparison of this relation with observations. In the active state, as the torus shrinks and uncovers the neutron star (see Fig. 9) the QPO frequency will increase, resulting in a positive I, ν correlation, as observed. In quiescence, we observe that when the intensity drops, the QPO frequency increases, indicating a decrease in the size of the thick disk region. These changes are all in the sense expected from a lower $\dot{M}$. However, once again geometrical effects would be expected to affect the conversion of I into $\dot{M}$, so that a direct comparison with the predicted $\dot{M}$, ν relation is not possible.

Optical and radio observations as well as X-ray observations of the iron line at 6.7 keV seem to be consistent with this picture. The optical flux is correlated with L_x in the active state and anticorrelated in quiescence (Canizares *et al.* 1975). Since the optical radiation is most probably reprocessed X-ray emission, shadowing of the outer disk by the thick inner disk can explain the observed optical variations. During the flaring episodes, the iron line intensity does not change (WPT). If this line is the result of recombination in an accretion disk corona then, its invariance also indicates that the X-ray continuum variations are caused by geometrical effects. Radio outbursts start only in X-ray quiescence (Miyamoto and Matsuoka 1977), when h/r is largest and the polar channel narrowest, which is when the most efficient particle acceleration might be expected. Whether the outer disk rim or the thick inner disk spans a greater angle as seen from the neutron star (cf. Milgrom 1978) may determine whether a system shows X-ray dips at the orbital period (e.g., White and Mason 1985) or QPO.

The weak LFN is in this scenario due to the low inclination of Sco X-1 ("pole-on" view), allowing the disk oscillations to cause a signal which gives equal positive and negative contributions to the total intensity. If the region which is periodically being occulted is fairly uniform in its X-ray emission properties, then suppression of the LFN follows automatically—no

"fine tuning" is required. In GX 5−1, a higher inclination would allow the thick disk oscillations to cause "net-nonzero" wave trains resulting in QPO–related LFN (for example, because the polar channel becomes completely obscured during part of the oscillation cycle). This higher inclination at the same time could prevent hard flaring: the disk would be always thick enough to intercept our line of sight to the neutron star.

GX 5−1 and Cyg X-2 also show two branched spectral behavior (Ponman 1982; Shibazaki and Mitsuda 1983; Branduardi *et al.* 1980), which is correlated with different QPO/LFN modes (van der Klis *et al.* 1985*c*; Hasinger *et al.* 1985). These might be explained in a similar way as considered here for Sco X-1, with any differences being due to the higher inclination and the smaller thick disk radii derived from the (usually) higher QPO frequencies.

VI. CONCLUSION

The QPO behavior of Sco X-1 is much more complex than that first reported from GX 5−1 and cannot without additional assumptions be explained by any of the models originally proposed for GX 5−1. The transitions we observe in Sco X-1 between the different QPO modes, and the direct relation between the QPO frequency and the blackbody luminosity, which holds for all states, both indicate that a single mechanism is responsible for the QPO properties seen in the two intensity states. We have explored the possibility of an obscuring oscillating disk model and find qualitative agreement with many of the observed X-ray spectral and fast timing characteristics of Sco X-1.

We thank the *EXOSAT Observatory* Team for their support. We thank Fred Lamb for discussions. The Laboratory for Space Research Leiden is supported financially by the Netherlands Organization for Pure Research (ZWO). We acknowledge useful discussions with participants at the Tenerife Workshop on Accretion onto Compact Objects (1986 April). We thank S. Andrews for infinite patience in typing and retyping the manuscript.

REFERENCES

Alpar, M. A., and Shaham, S. 1985, *Nature*, **316**, 239.
Angel, J., Kestenbaum, J., and Novick, R. 1971, *Ap. J.*, **169**, L57.
Berman, N. W., and Stollman, G. M. 1986, *Astr. Ap.*, **154**, L23.
Boyle, C. B., Fabian, A. C., and Guilbert, P. W. 1986, *Nature*, **319**, 648.
Branduardi, G., Kylafis, N. D., Lamb, D. Q., and Mason, K. O. 1980, *Ap. J. (Letters)*, **235**, L153.
Brinkman, A. C., Mewe, R., Langerwerf, T., Heise, J., Peacock, A., and White, N. E. 1985, *Space Sci. Rev.*, **40**, 201.
Canizares, C. R., Clark, G. W., Lewin, W. H. G., Schnopper, H. W., and Sprott, G. F. 1973, *Ap. J. (Letters)*, **179**, L1.
Canizares, C. R., *et al.* 1975, *Ap. J.*, **197**, 457.
Crampton, D., Cowley, A. P., Hutchings, J. B., and Kaat, C. 1976, *Ap. J.*, **207**, 907.
Deeter, J. E. 1984, *Ap. J.*, **281**, 482.
Ghosh, P., and Lamb, F. K. 1979, *Ap. J.*, **232**, 259.
Hameury, J. M., King, A. R., and Lasota, J. P. 1985, *Nature*, **317**, 597.
Hasinger, G., Langmeier, A., Sztajno, M., Trümper, J., Lewin, W. H. G., and White, N. E. 1986, *Nature*, **319**, 469.
Hasinger, G., Langmeier, A., Sztajno, M., Pietsch, W., and Gottwald, M. 1985, *IAU Circ.*, 4153.
King, A. R. 1985, *Nature*, **313**, 291.
Lamb, F. K., Shibazaki, N., Alpar, M. A., and Shaham, J. 1985, *Nature*, **317**, 681.
Lamb, P., and Sanford, P. W. 1979, *M.N.R.A.S.*, **188**, 555.
Lewin, W. H. G., van Paradijs, J., Jansen, F., van der Klis, M., Sztajno, M., and Trümper, J. E. 1985; *IAU Circ.*, 4101.
Lewin, W. H. G., *et al.* 1986, *IAU Circ.*, 4170.
Middleditch, J. 1985, talk presented at Workshop on Time Variability in X-Ray and Gamma-Ray Sources, Taos, NM.
Middleditch, J., and Priedhorsky, W. 1985, *IAU Circ.*, 4060 (MP85).
———. 1986, *Ap. J.*, **306**, 230 (MP86).
Milgrom, H. 1978, *Astr. Ap.*, **67**, L25.
Mitsuda, K., *et al.* 1985, *Pub. Astr. Soc. Japan*, **36**, 741.
Miyamoto, S., and Matsuoka, M. 1977, *Space Sci. Rev.*, **20**, 687.
Morfill, G. E., and Trümper, J. 1985, in *Proc. NATO-ARW Evolution of Galactic X-ray Binaries* (Reidel NATO ASI Series C 167), p. 173.
Patterson, J. 1981, *Ap. J. Suppl.*, **45**, 517.
Peacock, A., Andersen, R. D., Manzo, G., Taylor, B. G., Villa, G., Re, S., Ives, J. C., and Kellock, S. 1982, in *Proc. 15th ESLAB Symposium*, ed. R. D. Andersen (Dordrecht: Reidel), p. 525.
Pollock, A., *et al.* 1986, paper presented at Workshop on Accretion onto Compact Objects, Tenerife, Spain.
Ponman, T. 1982, *M.N.R.A.S.*, **201**, 769.
Priedhorsky, W. 1985, talk presented at Cambridge Discussion Meeting on *EXOSAT* Results.
———. 1986. *Ap. J. (Letters)*, **306**, L97.
Priedhorsky, W., Hasinger, G., Lewin, W. H. G., Middleditch, J., Parmar, A. N., Stella, L., and White, N. E. 1986, *Ap. J. (Letters)*, **306**, L91 (P86).
Pringle, J. E. 1981, *Ann. Rev. Astr. Ap.*, **19**, 137.
Shakura, N. I., and Sunyaev, R. A. 1973, *Astr. Ap.*, **24**, 337.
Shibazaki, N., and Mitsuda, K. 1983, in *Proc. Summer Workshop on Astrophysics*, Santa Cruz, (ISAS RN 234), p. 63.
Stella, L. 1986, in *Proc. Plasma Penetration into Magnetospheres*, ed. N. Kylafis, J. Papamastorakis, and J. Ventura (Crete: University of Crete Press), p. 199.
Stella, L., Parmar, A. N., and White, N. E. 1985, *IAU Circ.*, 4102.
Stella, L., Parmar, A. N., White, N. E., Lewin, W. H. G., and van Paradijs, J. 1985, *IAU Circ.*, 4110.
Stella, L., White, N. E., and Priedhorsky, W. 1985, *IAU Circ.*, 4117.
Tawara, Y., Hayakawa, S., Kunieda, H., Makino, F., and Nagase, F. 1982, *Nature*, **299**, 38.
Turner, M. J. L., Smith, A., and Zimmermann, H. U. 1981, *Space Sci. Rev.*, **30**, 513.
van den Heuvel, E. P. J., van Paradijs, J. A., and Taam, R. E. 1986, *Nature*, **322**, 153.
van der Klis, M. 1985, talk presented at Workshop on Time Variability in X-Ray and Gamma-Ray Sources, Taos, NM.
van der Klis, M., and Jansen, F. 1985*a*, in *Proc. NATO-ARW Evolution of Galactic X-ray Binaries* (Reidel NATO ASI Series C167), 129 (KJ85*a*).
———. 1985*b*, in *Proc. 4th Marcel Grossmann Meeting on Recent Developments in General Relativity*, in press (KJ85*b*).
van der Klis, M., Jansen, F., van Paradijs, J., Lewin, W. H. G., Trümper, J., and Sztajno, M. 1985*c*, *IAU Circ.*, 4140.
van der Klis, M., Jansen, F., van Paradijs, J., Lewin, W. H. G., van den Heuvel, E. P. J., Trümper, J. E., and Sztajno, M. 1985*a*, *Nature*, **316**, 225.
van der Klis, M., Jansen, F., White, N. E., and Stella, L. 1985*b*, *IAU Circ.*, 4068 (K85).
White, N. E., and Mason, K. O. 1985, *Space Sci. Rev.*, **40**, 167.
White, N. E., Mason, K. O., Sanford, P. W., Ilovaisky, S. A., and Chevalier, C. 1976, *M.N.R.A.S.*, **176**, 91.
White, N. E., Peacock, A., Hasinger, G., Mason, K. O., Manzo, G., Taylor, B. G., and Branduardi-Raymont, G. 1986, *M.N.R.A.S.*, **218**, 129.
White, N. E., Peacock, A., and Taylor, B. G. 1985, *Ap. J.*, **296**, 475 (WPT).

F. JANSEN: Laboratory for Space Research Leiden, Postbus 9504, 2300 RA Leiden, The Netherlands

A. N. PARMAR, L. STELLA, M. VAN DER KLIS, and N. WHITE: *EXOSAT Observatory*, Astrophysics Division, Space Science Department of ESA, ESTEC, Postbus 299, 2200 AG Noordwijk, The Netherlands